forests

MDPI

Article

Quantification of Root Systems and Soil Macropore Networks Association to Soil Saturated Hydraulic Conductivity in Forested Wetland Soils

Yinghu Zhang [1,2,3], Lu Wang [1,2,3], Wenqi Zhang [1,2,3], Zhenming Zhang [4] and Mingxiang Zhang [4,*]

[1] Co-Innovation Center for Sustainable Forestry in Southern China, Nanjing Forestry University, Nanjing 210037, China
[2] Jiangsu Provincial Key Laboratory of Soil Erosion and Ecological Restoration, Nanjing Forestry University, Nanjing 210037, China
[3] Priority Academic Program Development of Jiangsu High Education Institutions (PAPD), Nanjing Forestry University, Nanjing 210037, China
[4] School of Ecology and Nature Conservation, Beijing Forestry University, Qinghua East Road 35, Beijing 100083, China
* Correspondence: zhangmingxiang@bjfu.edu.cn

Abstract: Understanding the relationship between root systems, soil macropore networks, and soil hydraulic properties is important to better assess ecosystem health. In this study, treatments were performed in forested wetland soils with different vegetation densities, i.e., large (LWa) and small communities (LWb) of reed (*Phragmites australis* (Cav.) Trin. ex Steud.). At each plot, three undisturbed PVC cylinders (10 cm in diameter and 50 cm in height) were obtained, and X-ray microtomography (μCT) scanning was used to determine the root and macropore architectures. Results showed that the values of total root length and total root volume at LWa were significantly larger than those at LWb ($p < 0.05$). Imaged macroporosity, macropore volume, macropore length density, macropore node density, macropore branch density, mean macropore surface area, mean macropore diameter, and mean macropore volume at LWa were significantly larger than those at LWb ($p < 0.05$), whereas mean macropore length, mean macropore branch length, and mean macropore tortuosity at LWb were larger than those at LWa. Total root length and total root volume were positively correlated with soil saturated hydraulic conductivity. Imaged macroporosity, macropore volume, macropore length density, macropore node density, macropore branch density, mean macropore surface area, mean macropore diameter, and mean macropore volume were positively correlated with soil saturated hydraulic conductivity, whereas mean macropore length, mean macropore branch length, and mean macropore tortuosity were negatively correlated with soil saturated hydraulic conductivity. In conclusion, root systems and soil macropore networks constitute a complex synthesis inside soil environments, and together affect soil hydrological responses.

Keywords: root systems; soil macropores; soil saturated hydraulic conductivity; Yellow River Delta

Citation: Zhang, Y.; Wang, L.; Zhang, W.; Zhang, Z.; Zhang, M. Quantification of Root Systems and Soil Macropore Networks Association to Soil Saturated Hydraulic Conductivity in Forested Wetland Soils. *Forests* **2023**, *14*, 132. https://doi.org/10.3390/f14010132

Academic Editor: Thomas H. DeLuca

Received: 16 November 2022
Revised: 7 January 2023
Accepted: 10 January 2023
Published: 11 January 2023

1. Introduction

The Yellow River Delta is one of the most active deltas in China [1]. Forested wetland is an important component in this area, which shows positive influences on soil and water conservation, ecological functions, and vegetation interactions with soil erodibility [2,3]. However, during the last several decades, the delta has experienced environmental changes, such as agricultural exploration, expansion of the urban residential area, vegetation degradation, and petroleum refining, which result in deterioration of the structure and function of the wetland ecosystems [4]. For example, the overexploitation of petroleum in the delta can cause a series of environmental problems. The petroleum that is retained in the soils cannot be removed by the power of nature. Further, it can be transported efficiently through soil macropores to the groundwater levels. In particular, more soil fissures could be developed

due to the serious degradation of forested wetland. Therefore, it is vital to develop a common method to restore the degraded wetland. Reed is one of the most widely distributed dominant species in the Yellow River Delta. Reed community is widely distributed in coastal marshes with shallow groundwater depth. It can withstand and present different ecological characteristics with different water and salt habitat conditions. Reed plays an important role in forested wetland ecosystems [5] due to its purification of wastewater and its accumulation of nutrients. Reed is used in the restoration and reconstruction of wetland ecosystems. Root systems of reed are the interface between aboveground vegetation and belowground soils. They can not only support vegetation growth by absorbing water, minerals, and nutrients from the soils, but they also form more root channels during their decomposition. However, in different stages of wetland restoration, how the root systems of reed community interact with the surrounding soils (i.e., soil macropores) is still unclear.

Soil macropores formed by root systems are a major factor influencing water flow and solute transport [1]. The interaction between root systems and soil macropores is increasingly studied [4,6–8]. Most studies quantifying the interaction between root systems and soil macropores have shown that root systems can promote the formation of soil macropores and increase soil microporosity [7]. For example, Bodner et al. [9] concluded that coarse root systems increased macroporosity (larger than 37.5 µm in diameter) by 30%, and root biomass increased soil macropore area and length. Hu et al. [7] found that a large number of soil macropores in soils can be attributed to the greater development of root systems. Root systems affect soil macropore architecture through mechanical intercalation and by squeezing the surrounding soils during the intercalation processes [10]. Therefore, understanding the interaction between root systems, soil macropores, and soil hydrology could provide more information for the development of degraded wetlands. Root systems and soil macropore networks play crucial roles in soil hydrological responses, such as soil hydraulic conductivity [11]. Soil hydraulic conductivity, which determines the ability of soil to conduct water, is an important soil hydraulic property influencing water flow and solute transport [12]. Soil hydraulic conductivity is of ecological and hydrological significance. Soil hydraulic conductivity is strongly dependent on root systems and soil macropores [13]. Previous studies have been designed to confirm soil hydraulic conductivity by characterizing the geometry of soil macropore spaces including macropore distribution, macropore tortuosity, and other macropore attributes [13]. For example, the impact of soil macropores on soil hydraulic conductivity depends on their arrangement and 3D characteristics including macropore length, volume, surface area, and mean tortuosity [14,15]. Despite there being some research available about soil hydraulic conductivity development under different land uses, such as grassland, cultivated lands, shrub areas, and forest-covered soils [13,16–18], there are very limited data about the development of soil hydraulic conductivity in degraded soils. There exists a large body of evidence that wetland degradation can promote soil fissure development. Soil fissures such as soil macropores can impact hydrological responses. Particularly, pollutants and other contaminants carried by water can be transported from the soil surface to groundwater levels via those soil fissures, which further threaten soil ecology and hydrology [19]. We hypothesize that the density of root systems can lead to different attributes of soil macropores, and they can together impact soil hydrological responses. However, less explored is the relationship between root systems and soil macropores, and their joint effects on soil hydraulic conductivity in degraded soils. In this study, we mainly evaluated (1) the visualization of the three-dimensional structure of root systems and soil macropore networks, (2) the correlation between root systems and soil macropore parameters (imaged macroporosity, macropore volume, macropore length density, macropore node density, macropore branch density, mean macropore surface area, mean macropore diameter, mean macropore volume, mean macropore length, mean macropore branch length, and mean macropore tortuosity), and (3) the effects of root systems and soil macropores on soil saturated hydraulic conductivity.

2. Materials and Methods

2.1. Study Area

The study area is located in the Yellow River Delta National Natural Reserve (118°32.981′–119°20.450′ E, 37°34.768′–38°12.310′ N) in northeastern Shandong Province, China (Figure 1). The Yellow River Delta National Natural Reserve covers an area of 153 km^2. The main landform types in the study area comprise a land zone, tidal flat zone, and subtidal zone. The climate is warm-temperate continental with a mean annual precipitation of 576.7 mm, mean annual potential evapotranspiration of 1962 mm, and mean annual temperature of 12.1 °C. The frost-free period is 196 d [20]. The study area's main soil texture is determined by soil particle size classification developed by the U.S. Department of Agriculture (USDA). Based on the USDA system, soil particle sizes in the study area are divided into three groups: sand, silt, and clay. Soil texture in the area is sandy silt, and soil types are fluvo-aquic and saline soils formed by the Yellow River's alluvial deposits (Table 1). The three main vegetation types are deciduous broad-leaved forests, marsh vegetation, and salt-bearing vegetation. The dominant vegetation is locust (*Robinia pseudoacacia* L.) in the deciduous broad-leaved forest communities, reed in marsh vegetation communities, and tamarisk (*Tamarix chinensis*) and seepweed (*Suaeda glauca*) in the salt-bearing vegetation communities [20].

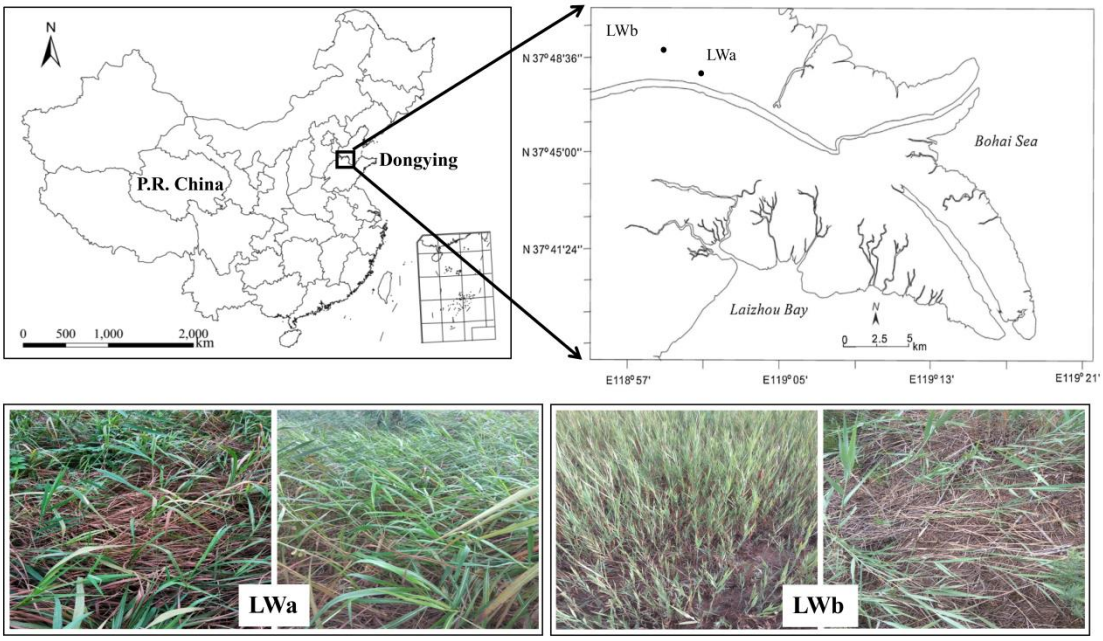

Figure 1. Location of the study area.

Table 1. Soil properties at each soil depth at LWa and LWb.

Plots	Soil Depth (cm)	Total Soil Porosity (%)	Soil Capillary Porosity (%)	Soil Non-Capillary Porosity (%)	Sand	Silt	Clay	Soil Bulk Density (g/cm^3)	Soil Organic Matter (g/kg)	Soil Total Nitrogen (g/kg)	Soil Total Phosphorus (g/kg)	Soil Available Phosphorus (mg/kg)
LWa	0–10	0.563 ± 0.024	0.520 ± 0.049	0.043 ± 0.037	0.211 ± 0.082	0.563 ± 0.115	0.226 ± 0.044	0.912 ± 0.094	21.039 ± 9.265	1.345 ± 0.631	0.614 ± 0.033	3.927 ± 1.933
	10–20	0.483 ± 0.011	0.468 ± 0.010	0.014 ± 0.008	0.170 ± 0.041	0.623 ± 0.123	0.207 ± 0.135	1.304 ± 0.052	5.050 ± 0.503	0.358 ± 0.043	0.569 ± 0.055	2.398 ± 1.031
	20–40	0.479 ± 0.016	0.471 ± 0.012	0.009 ± 0.005	0.327 ± 0.120	0.561 ± 0.122	0.112 ± 0.032	1.384 ± 0.002	3.857 ± 1.257	0.270 ± 0.094	0.538 ± 0.045	1.792 ± 0.111
	40–60	0.464 ± 0.029	0.454 ± 0.021	0.011 ± 0.015	0.521 ± 0.130	0.413 ± 0.127	0.067 ± 0.006	1.427 ± 0.177	2.692 ± 0.709	0.183 ± 0.039	0.518 ± 0.038	1.655 ± 0.231

Table 1. *Cont.*

Plots	Soil Depth (cm)	Total Soil Porosity (%)	Soil Capillary Porosity (%)	Soil Non-Capillary Porosity (%)	Sand	Silt	Clay	Soil Bulk Density (g/cm^3)	Soil Organic Matter (g/kg)	Soil Total Nitrogen (g/kg)	Soil Total Phosphorus (g/kg)	Soil Available Phosphorus (mg/kg)
LWb	0–10	0.478 ± 0.016	0.472 ± 0.015	0.006 ± 0.002	0.202 ± 0.053	0.669 ± 0.069	0.129 ± 0.019	1.406 ± 0.061	11.244 ± 2.839	0.694 ± 0.038	0.694 ± 0.073	3.576 ± 0.279
	10–20	0.468 ± 0.017	0.463 ± 0.016	0.004 ± 0.001	0.193 ± 0.071	0.688 ± 0.077	0.113 ± 0.007	1.388 ± 0.021	2.781 ± 0.693	0.200 ± 0.033	0.582 ± 0.003	1.749 ± 0.181
	20–40	0.468 ± 0.013	0.461 ± 0.018	0.007 ± 0.005	0.387 ± 0.067	0.542 ± 0.060	0.071 ± 0.010	1.418 ± 0.039	2.535 ± 1.072	0.159 ± 0.073	0.584 ± 0.021	2.552 ± 0.746
	40–60	0.491 ± 0.006	0.490 ± 0.005	0.001 ± 0.001	0.243 ± 0.172	0.656 ± 0.145	0.101 ± 0.036	1.467 ± 0.058	2.126 ± 1.340	0.188 ± 0.052	0.576 ± 0.027	2.781 ± 0.292

2.2. Soil Sampling

In the wet season of July 2017, the reed treatment was conducted at the sampling plots. In addition, all the plots for the LWa (large) and LWb (small) communities of reed treatments were located at the same plot and had similar soil properties. Due to alluvial deposits from the upstream of the Yellow River, there is no soil spatial variability in the sampling plots, and we therefore excavated a total of 6 PVC samples across plots. In our study, LWa represents areas with high vegetation cover (98%) and height (2.0 m), whereas LWb represents areas with low vegetation cover (30%) and height (0.6 m). Soil sampling locations were randomly selected at each treatment due to few spatial variabilities in soil properties. Undisturbed soil columns using PVC cylinders (4 mm wall thickness, 10 cm in diameter, and 50 cm in height) with three replicates were extracted vertically from the soil profiles at the depths of 0–50 cm at each sampling plot. We moistened the soils with water before sampling [7]. The excavation procedure of those undisturbed soil columns, using PVC cylinders to avoid damage to the soil structure during soil sampling, was as follows: (1) the aboveground reeds were carefully clipped and the litter was completely removed carefully with minimal disturbance; (2) a large pit was dug in the experimental plots using a pick; (3) the soil clod was carved carefully with small shovels and hand tools, and the roots were cut with pliers; (4) four vertical lateral sides were excavated, and then cylindrical-shaped soil sides were excavated with small shovels; (5) the top surfaces of the PVC cylinders were prepared carefully with a knife and cleaned with a brush to remove loose soil particles resulting from digging; (6) the soil column was trimmed at the bottom, and the bottom was sealed with plastic film and cloth; and (7) the soil column excavated by the PVC cylinders was tightened with iron wire and then transported carefully [21]. The cylinders were placed into a box and wrapped with sponge to prevent crushing. Six soil columns were collected in this study and transported from the field to the laboratory for X-ray CT scanning. Soil water content of the undisturbed soil columns can influence the threshold values used for the image segmentation. The soil columns from different experimental plots were taken at different times with different initial soil water content. Therefore, each soil column must be wetted before X-ray CT scanning to minimize the variability of initial soil water content. By ponding water at the top surface of each soil column and draining with the bottom of the column open to the atmosphere for 3 days, we made the initial soil water content more consistent [22].

2.3. CT Scanning and Macropore Data Acquisition

The industrial CT has a higher resolution compared with the medical CT. The undisturbed soil columns were scanned with an industrial X-ray CT. The scanning parameters were as follows: resolution of 0.05 mm, voltage of 150 kV, and current of 480 µA. The CT scanning mode was sequential, the scanning spacing between projections was 0.1 mm, and 4200 slices were obtained from each soil column (Figure 2). VGStudio MAX (software VGStudio MAX 2.2, Volume Graphics company, Germany) was utilized to reconstruct the

scanned images. All images were transformed from 16-bit images to 8-bit images for later processing. The region of interest was selected to exclude the voids near the soil column walls and to minimize the effects of beam hardening [22].

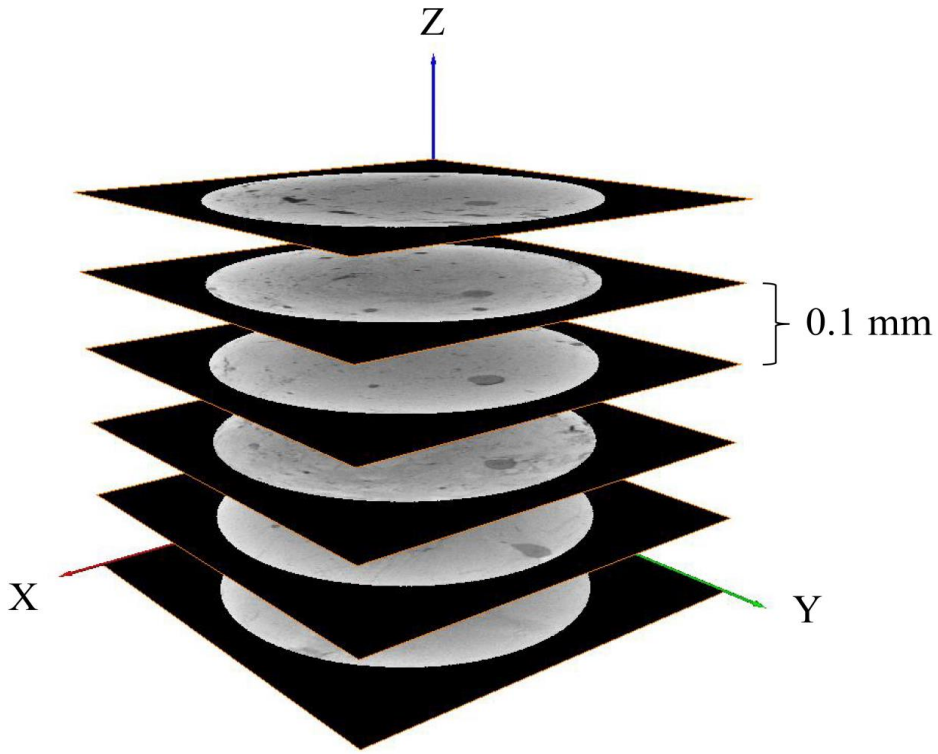

Figure 2. Slices obtained from whole soil columns.

To reduce the negative influences of noise and brightness variation before image segmentation, the normalize and the 3D median filter plugins were activated in the ImageJ software. The normalize plugins recalculate the grey levels of images to make the brightness of the grey images consistent. The 3D median filter can reduce the noise of the grey images [23]. Afterwards, all CT images were resampled using Avizo (software Avizo 9.0, the Victor Smorgon Group company, Australia). We determined the threshold values of the soil macropores to a depth of 50 cm in the sampling sites to acquire some binary images using a manually created macropore [7]. The threshold values of soil macropores (larger than 0.05 mm in diameter) were obtained following Hu et al. [7] (Figure 3). A manually created macropore (Plexiglas cylinder) with a known diameter measured by a digital caliper was inserted into an undisturbed soil column and then removed from the column. The column was then scanned by X-ray CT. We selected the upper, middle, and lower parts of the Plexiglas cylinder, respectively. First, we assumed a threshold value for the thresholding sample, and then calculated the soil macropore size based on the image analysis [7]. Then, we compared the calculated size of the soil macropore with the actual macropore size determined by a digital caliper. If the difference was >1%, the threshold value was reset until the calculated and actual size of the soil macropore were the same [7]. If the difference between the calculated and actual diameters of the soil macropores was within 1%, it was regarded as the threshold value. Using the threshold value, the images were translated into binary images. In the binary images, the black areas are soil macropores, and the white areas are the soil matrix [7].

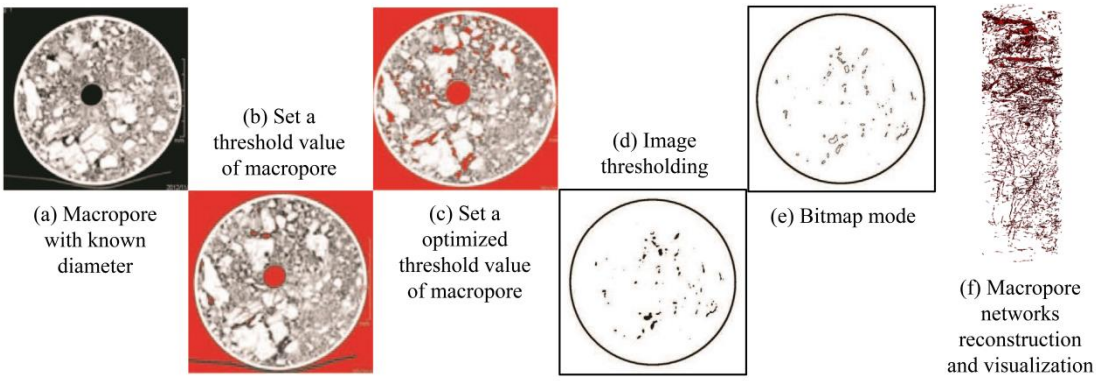

Figure 3. The process of reconstruction and visualization of soil macropores [22].

After segmentation, three-dimensional architectures of soil macropores were reconstructed by Avizo 9.0 software [7]. Soil macroporosity, mean diameter, mean surface area, network density, length density, node density, branch density, mean length, and mean branch length were determined using the Avizo 9.0 software module 'Label Analysis'. The mean tortuosity was evaluated using the Avizo 9.0 software module 'Centroid Path Tortuosity'. The volume (V_p) was evaluated using the Avizo 9.0 software module 'Volume Fraction' [24]. Since soil macropores are three-dimensional, the skeletonization of soil macropores was considered to determine the topology and length of the soil macropores and to reconstruct the soil macropore networks. A network of one soil macropore may include several branches of connected soil macropores or just one individual soil macropore [25]. The specific procedures used in this study for characterization of soil macropore networks are referenced to Luo et al. [25] and Hu et al. [7].

$$P = \frac{V_p}{V_t} \tag{1}$$

where P(%) is soil macroporosity, V_p is the soil macropore volume of the region of interest (mm^3), and V_t is the total sample volume of the region of interest (mm^3).

$$\rho_d = \frac{N_d}{V_t} \tag{2}$$

where ρ_d is the soil macropore network density (number, mm^{-3}), and N_d is the number of soil macropore networks.

$$\rho_n = \frac{N_n}{V_t} \tag{3}$$

where ρ_n is the soil macropore node density (number, mm^{-3}), and N_n is the number of soil macropore nodes.

$$\rho_t = \frac{L_t}{V_t} \tag{4}$$

where ρ_t is the soil macropore length density (mm, mm^{-3}), and L_t is the total actual length of soil macropores (mm).

$$L_t = \frac{V_p}{S} \tag{5}$$

where S is the soil macropore surface area (mm^2).

$$\tau = \frac{L_t}{L_l} \tag{6}$$

where τ is the soil macropore tortuosity, and L_l is the total straight-line distance of all the soil macropores in the total sample (mm).

$$\overline{\tau} = \frac{\sum_{i=1}^{n} L_{ti}}{\sum_{i=1}^{n} L_{li}} \quad (7)$$

where $\overline{\tau}$ is the mean soil macropore tortuosity, i is the index of a soil macropore branch, and n is the total number of soil macropore branches [25].

2.4. Root Systems Data Acquisition

The threshold values were considered to distinguish among soil macropores, root systems, and solid phases. In order to avoid selecting most of the impurities (i.e., soil mineral particles, soil organic matter, and microorganisms), we took advantage of the magic wand tool in the Avizo 9.0 software to select roots in the two-dimensional images (Figure 4). The tool was also applied to all slices. Meanwhile, the visualization of root systems was shown in the visual window [13]. If the selected root space did not match the measured root volume and surface, we enlarged the selected area to make it match better. If the enlarged root area of a two-dimensional slice included unnecessary parts at the edge of the root systems, all slice voxels were shrunk until the selected area reached a reasonable area [13]. If a root was not continuous in a single soil column sample, another root spot was selected in the two-dimensional slice until all root systems were traced. After segmentation and binarization, the visualization of root systems was obtained. Since root systems are 3D, skeletonization of root systems is necessary to effectively visualize the root networks in 3D [26] and accurately calculate the root system parameters (i.e., total root length and total root volume) [7]. Skeletonization of 3D root networks can improve the quantification of length-based root system parameters [25] and show the connectivity among root systems [27]. Many root systems in large soil columns may have dead ends; therefore, the skeletons of root systems with dead ends could be accurately calculated. The skeleton of a root is its central line, from which the distance is the closest to more than one boundary point [25].

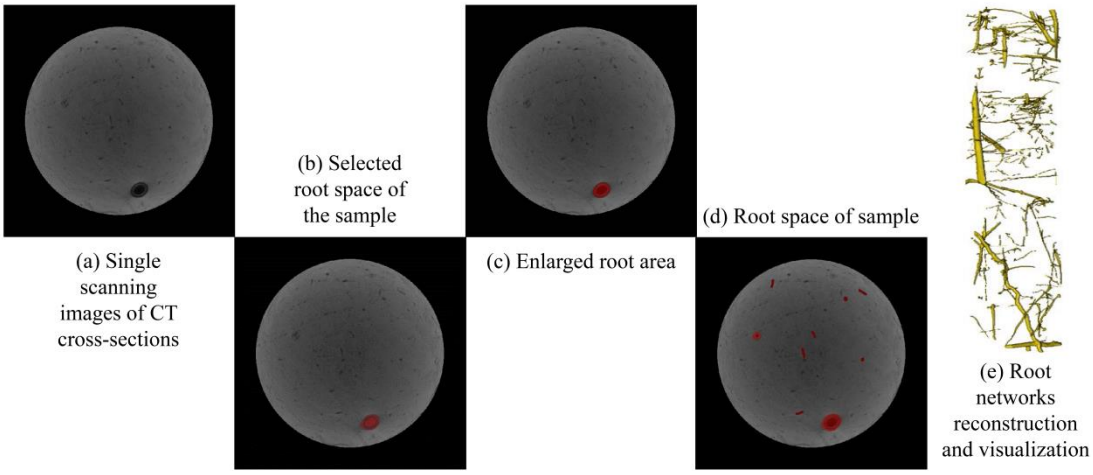

Figure 4. The process of reconstruction and visualization of root systems [13].

2.5. Determination of Soil Saturated Hydraulic Conductivity (Ks)

Using a ring knife at different soil depths (0–10, 10–20, 20–40, and 40–60 cm), undisturbed soil columns were excavated from the soil profiles and placed in water for 24 h. During soaking, the water surface was kept level with the upper mouth of the ring knife, and water was not allowed to flood the soil surface of the upper mouth of the ring knife. The ring knife was removed at a predetermined time, an empty ring knife put on, and the ring knife placed on the funnel, which was covered with a beaker. Water was added

to the empty ring knife above, so the water surface was 1 mm lower than the ring knife edge, and 2 cm below the water layer. After adding water, a stopwatch was used to time the first drop of water from the funnel. The beaker under the funnel was replaced every 1, 2, 3, 5, and 10 min. The interval time depended on the speed of water infiltration. A measuring cylinder was used to measure the amount of water seepage. The test lasted until the amount of water outflow was equal in unit time.

Darcy's law was used to determine K_s, as below [28].

$$Q = K_s \times i \times A \tag{8}$$

where Q is the flow rate at steady conditions in ml/min, K_s is the soil saturated hydraulic conductivity in cm/min, A is the cross-sectional area of the soil column in cm^2 (equal to 38.5 cm^2 for a soil column of 7 cm diameter), and i is the hydraulic gradient as follows:

$$i = \frac{\Delta H}{L} \tag{9}$$

where ΔH is the difference between the soil hydraulic head on the soil surface and bottom of the soil column in cm, and L is the length of the soil column in cm. In this study, the value of L was 10 cm. The flow rate was the effluent volume divided by time. Finally, soil saturated hydraulic conductivity was calculated as follows:

$$K_S = \frac{\Delta V}{\Delta T \times i \times A} \tag{10}$$

where ΔV is the volume of the outflow, and ΔT is the time step.

2.6. Statistical Analysis

All statistical analyses were conducted using SPSS 22.0 software. Differences among the measured root and soil macropore parameters between the different sampling sites were analyzed using the least significant difference (LSD) test. Statistical significance was determined at $p < 0.05$ level to quantify the relationship between root systems, soil macropores, and soil saturated hydraulic conductivity.

3. Results

3.1. Characterization between Root Systems and Soil Macropores

The 3D visualizations of root and macropore networks in sampling sites are shown in Figure 5. The total root length and volume in the region of interest at the depths of 0–50 cm were 15,100 ± 3125 mm and 78,100 ± 2136 mm^3 at LWa and 8900 ± 921 mm and 12,800 ± 3162 mm^3 at LWb. The correlations between the estimated total root length and total root volume determined by X-ray CT and those determined by the standard root systems washing method are shown in Figure 6. The results showed that X-ray CT is a suitable method for root system characterization. Root system density in LWa non-compacted soils was distinctly richer than that in LWb compacted soils ($p < 0.05$) (Figure 7).

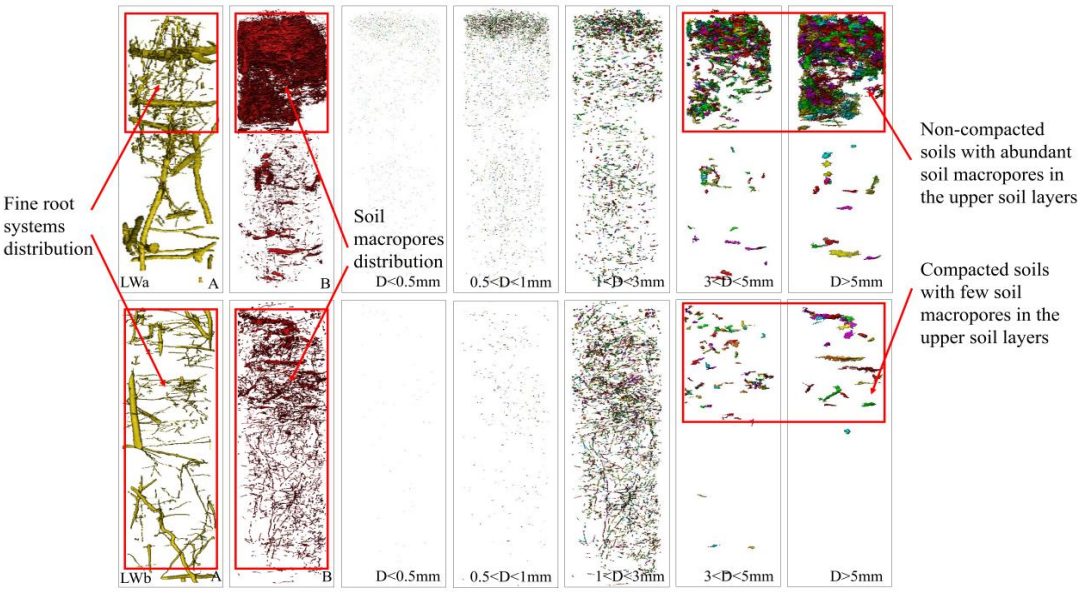

Figure 5. Three-dimensional structure of the root and macropore networks at LWa and LWb (A represents the 3D structure of root systems, B represents the 3D structure of soil macropores, and D represents equivalent diameter).

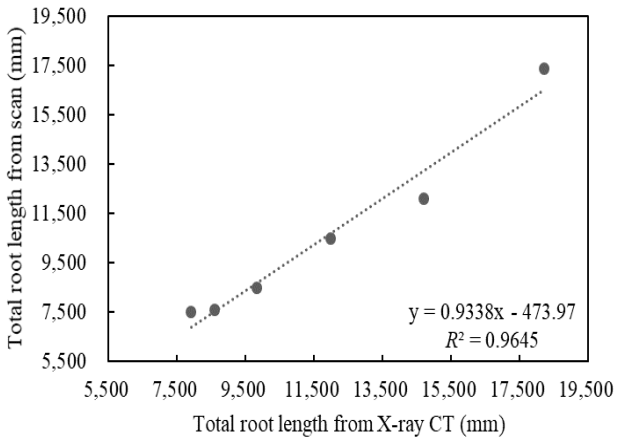

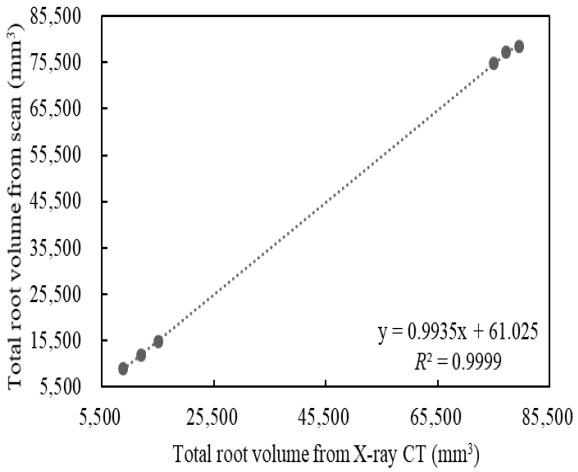

Figure 6. Comparisons between total root length and total root volume determined by X-ray CT and root system scanning after water washing.

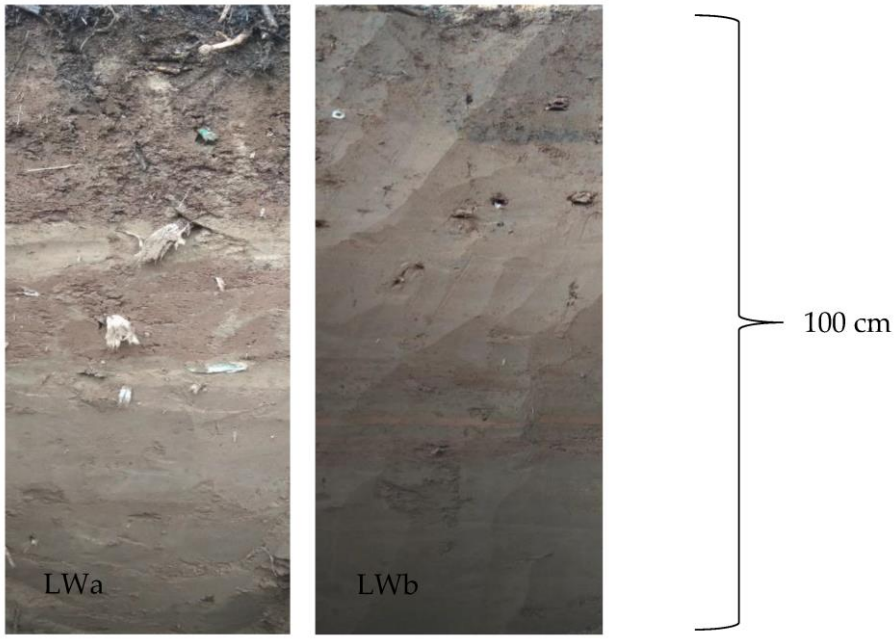

Figure 7. Photographs of sampling site soil profiles.

The number of soil macropores was considerably higher at LWa than at LWb (Table 2). The LWa in the region of interest at the depths of 0–50 cm had a comparatively higher imaged macroporosity (larger than 0.05 mm in diameter) (0.021 ± 0.007 mm^3 mm^{-3}), macropore total volume ($10.3 \times 10^4 \pm 6132$ mm^3), length density ($45.5 \times 10^4 \pm 11{,}026$ mm m^{-3}), node density ($11.3 \times 10^4 \pm 4031$ number m^{-3}), branch density ($10.2 \times 10^4 \pm 5121$ number m^{-3}), mean surface area (32.1 ± 10.2 mm^2), mean diameter (2.9 ± 0.8 mm), and mean volume (5.6 ± 1.3 mm^3) than LWb (0.005 ± 0.002 mm^3 mm^{-3}, $1.5 \times 10^4 \pm 3021$ mm^3, $1.8 \times 10^4 \pm 2957$ mm m^{-3}, $0.7 \times 10^4 \pm 1275$ mm m^{-3}, $0.08 \times 10^4 \pm 215$ number m^{-3}, 14.7 ± 3.6 mm^2, 1.5 ± 0.6 mm, and 3.6 ± 1.1 mm^3). In contrast, the LWa in the region of interest at the depths of 0–50 cm had a comparatively lower macropore mean length (180.3 ± 36.2 mm), branch length (205.2 ± 70.2 mm), and tortuosity (1.1 ± 0.5) than LWb (416.9 ± 120.1 mm, 444.5 ± 90.5 mm, and 1.2 ± 0.5).

Table 2. Number of soil macropores in entire soil columns at LWa and LWb.

Plots	Equivalent Diameter (mm)	Number of Soil Macropores
LWa	0.05 < D < 0.5	7072 ± 562 ^{aA}
	0.5 < D < 1	6502 ± 783 ^{aA}
	1 < D < 3	2837 ± 612 ^{aB}
	3 < D < 5	772 ± 122 ^{aC}
	D > 5	505 ± 101 ^{aC}
LWb	0.05 < D < 0.5	280 ± 92 ^{bC}
	0.5 < D < 1	454 ± 68 ^{bB}
	1 < D < 3	3383 ± 534 ^{aA}
	3 < D < 5	84 ± 10 ^{bD}
	D > 5	22 ± 12 ^{bE}

Lowercase letters represent the significant difference in number of soil macropores with the same diameter between LWa and LWb; capital letters represent the significant difference in number of soil macropores between different diameters at the same site.

The results of the correlation analyses between root systems and soil macropores are shown in Figure 8. Total root length and total root volume were positively correlated with imaged macroporosity, macropore volume, length density, node density, branch density, mean macropore surface area, mean macropore diameter, and mean macropore volume,

whereas they were negatively correlated with mean macropore length, mean macropore branch length, and mean macropore tortuosity.

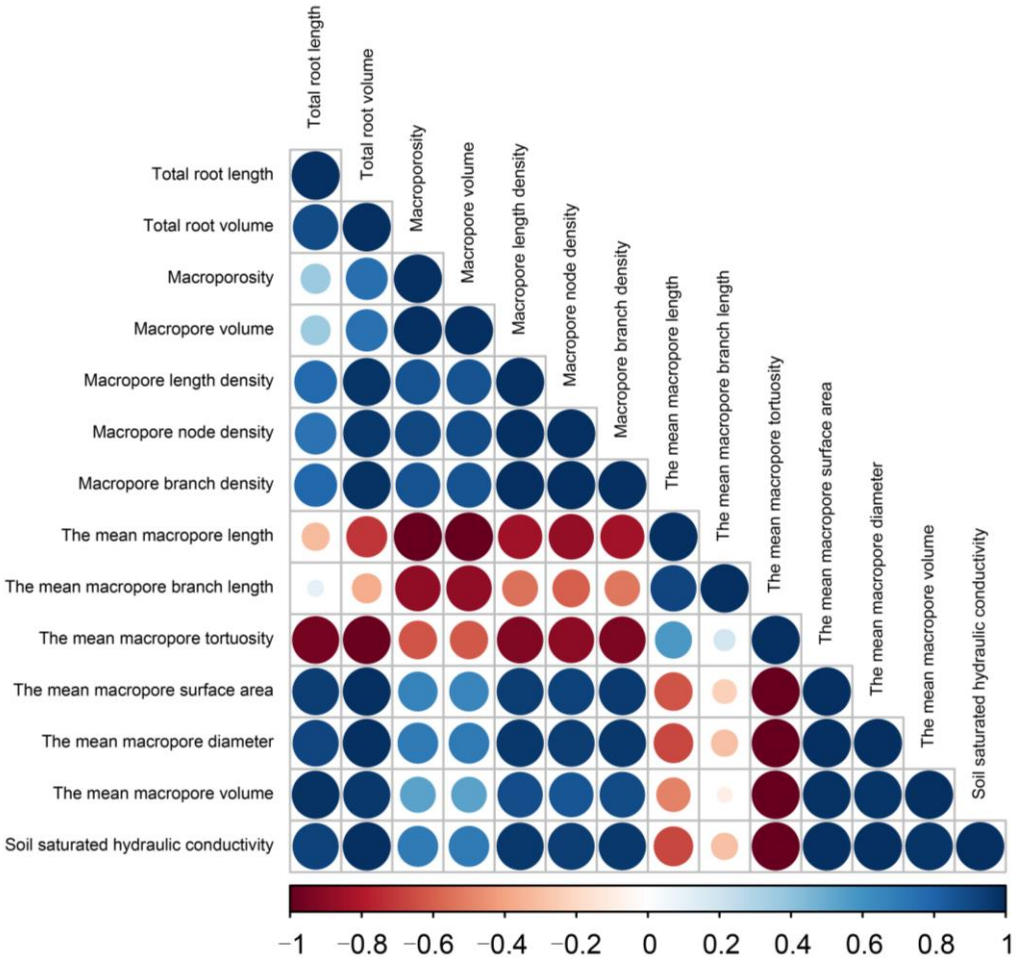

Figure 8. The correlation analyses between root systems, soil macropores, and soil saturated hydraulic conductivity.

3.2. Quantification between Root Systems, Soil Macropores, and Soil Saturated Hydraulic Conductivity

Of all the soil columns studied, soil saturated hydraulic conductivity at each soil depth was significantly greater at LWa (7.38 ± 2.28 cm/h at 0–10 cm, 0.72 ± 0.60 cm/h at 10–20 cm, 0.54 ± 0.48 cm/h at 20–40 cm, and 0.42 ± 0.36 cm/h at 40–60 cm) than that at LWb (0.29 ± 0.35 cm/h at 0–10 cm, 0.60 ± 0.46 cm/h at 10–20 cm, 1.20 ± 0.67 mL/min at 20–40 cm, 0.26 ± 0.40 cm/h at 40–60 cm).

Figure 8 depicts the relationship between root systems, soil macropores, and soil saturated hydraulic conductivity. The correlation analysis results shown in Figure 8 indicate that total root length and total root volume are positively correlated with soil saturated hydraulic conductivity. The correlation analysis results indicated in Figure 8 show that imaged macroporosity, macropore volume, macropore length density, macropore node density, macropore branch density, mean macropore surface area, mean macropore diameter, and mean macropore volume are positively correlated with soil saturated hydraulic conductivity, whereas mean macropore length, mean macropore branch length, and mean macropore tortuosity are negatively correlated with soil saturated hydraulic conductivity.

4. Discussion

4.1. Effects of Forested Wetland Conditions on Root Systems Distribution

More roots were located at LWa than at LWb. This is in contrast to research suggesting that increased soil bulk density in compacted soils can increase total root length due to the increased production of fine root systems to facilitate the acquisition of soil resources [29]. However, some studies indicated that soil compaction can generally have a negative effect on total root length and elongation [30,31]. Compacted soils at the LWb site may increase root systems penetration resistance [32] and affect their clustering [33]. Root length decreased in compacted soils [32–34]. This is because root system growth can be restricted by the penetration resistance of soils [35]. Furthermore, low soil nutrients at LWb also restrict root development [36,37]. For LWa with non-compacted soils, the root systems were thicker and more fibrous (Figure 5), which is consistent with the results of Kristoffersen and Riley [38]. This is because non-compacted soils at LWa have a large number of coarse soil macropores (Figure 5). Those walls of soil macropores are richer in soil nutrients than the surrounding soil matrix. Root systems can grow into those soil macropores or along the walls of soil macropores without any resistance [39]. However, this is in contrast to the study by Wang et al. [40]. They confirmed that soil compaction increased the average diameter of root systems, indicating that soil compaction made root systems thicker. In our study, a better soil physical-chemical condition at LWa can provide a suitable environment for the balance and development of forested wetland ecosystems. It can be regarded as a sink of soil nutrients and water resources, which can be beneficial for the root systems.

4.2. Effects of Forested Wetland Conditions on Soil Macropores

Values of most attributes of soil macropores were richer at LWa than at LWb. The findings could be explained by the fact that the presence of abundant root systems at LWa improved soil macropore structure and increased macropore density [7,11,27]. In contrast, the few root systems at LWb would not protect soil macropore structure, which results in higher macropore tortuosity at LWb [7] and decreased macroporosity and number of soil macropores [27]. Higher soil bulk density at LWb leads to the loss of soil macropores [41]. There is a complex relationship between root systems and soil macropores. These results are consistent with those of Hu et al. [13]. In their study, they confirmed that root density was significantly and positively correlated with imaged macroporosity, macropore surface area density, length density, node density, and branch density [13]. In another study, Kochiieru et al. [1] also confirmed that root volume is significantly correlated with the volume of fine and very fine soil macropores, but they concluded that root length density is positively correlated with the volume of very fine soil macropores. A positive correlation between root system parameters and most attributes of macropores was revealed in our study, which indicates that root systems have a significant effect on soil macropore development [42]. Root systems with high total length and volume have a high degree of lignification [43]. The surface of root systems may have been sufficiently rough, which can result in the formation of soil macropores between the rough root surface and surrounding soils. The rough convexity of root systems' surface increased the disturbance to the surrounding soils during the stretching and thickening processes of root systems [43]. It is possible that root systems with high total length and volume may generate large air gaps between the root and surrounding soils [9]. Root systems with high stiffness induce strong movement of soil particles, which can increase the interaggregate void space [43]. In addition, the disruption of macroaggregates due to the shifting of root systems may also form new pores inside the aggregate, which can increase the number and volume of soil macropores as well as other attributes of soil macropores. Root systems can modify soil macropore networks by different mechanisms, such as translocating soil aggregates, increasing soil aggregation through root exudates and related biological activities, and root decomposition [42]. However, there remains many soil macropores that do not contain root systems in our experimental data (Figure 5). It is possible that soil macropores are not continuously connected to the soil surface or that root system architecture in the soil surface cannot facilitate soil macropore

location [42,44]. Therefore, a healthy forested wetland ecosystem can make the soils more ventilated. The favorable environments in the forested wetland can facilitate the turnover process of soil nutrients and cycling of other organisms in the ecosystems. The beneficial environments can also increase the connectivity of soils so as to make soil pores more effective in soil functions.

4.3. Effects of Forested Wetland Conditions on Soil Saturated Hydraulic Conductivity

In the LWb soil depth 20–40 cm, the sandy loam layer is characterized by higher soil saturated hydraulic conductivity compared with other soil layers, which is consistent with the results of Jiang et al. [45]. In the LWb soil depth 20–40 cm, the sand content dramatically increases, and the silt content reduces compared with other soil layers. With an increase in sand content, the number of soil macropores will increase, which results in increased soil saturated hydraulic conductivity [16].

In our study, total root length and volume are positively correlated with soil saturated hydraulic conductivity. These results are consistent with Shi et al. [46] and Zhu et al. [47]. Soil hydraulic conductivity is altered particularly within soils where root systems are concentrated. Specifically, root length and median root radius are the best predictors for soil hydraulic conductivity changes [48]. A close positive relationship between total root length and soil hydraulic conductivity was observed, indicating that higher soil hydraulic conductivity could be attributed to larger total root length [49]. The positive correlation between root volume and soil hydraulic conductivity suggests that root volume is also important in increasing soil hydraulic conductivity [16]. Coarse root systems are likely to increase soil saturated hydraulic conductivity via the formation and development of soil macropores through the amalgamation of soil particles into soil aggregates and root channels during their decomposition [47,50]. Furthermore, the expansion of coarse root systems is likely to cause compression of soil particles [50], which also promotes the formation of soil macropores and increased soil saturated hydraulic conductivity [47]. However, fine root systems at low density can clog soil pores during their growth, whereas fine root systems at high density tend to eliminate soil macropore volume, so both fine root systems can lead to reduced soil saturated hydraulic conductivity [50]. For example, Archer et al. [16] confirmed that coarse root systems can promote soil hydraulic conductivity. This is because coarse root systems are older than fine root systems, and they will shrink and expand their root branching with time [51]. Such physical movement can create conduits for preferential water flow and solute transport [48]. The presence of such conduits could increase soil hydraulic conductivity [52]. During the establishment of root systems, soil hydraulic conductivity can decrease as root systems fill the soil macropores. Over time, soil hydraulic conductivity can increase as root systems begin to die back. Finally, an equilibrium point is reached when root systems fill those old root channels, which results in higher soil hydraulic conductivity [16]. However, some studies confirmed that root systems within a specific range of diameters from 0.5 mm to 2 mm played an important role in soil hydraulic conductivity, whereas root systems with notably smaller or larger diameters may have less effect on soil hydraulic conductivity [46]. Furthermore, the enhancement of soil saturated hydraulic conductivity because of root systems can be expected in fine-textured soils [50]. Overall, the positive correlation between total root length, total root volume, and soil saturated hydraulic conductivity may be attributed to two aspects. Firstly, due to root system growth and decomposition, well-connected large soil macropores or root channels were formed, which can directly increase soil saturated hydraulic conductivity [53,54]. Secondly, root systems can increase total soil porosity via binding and bonding soil particles [55], and can also improve soil structure by releasing soil exudates and increasing soil organic matter content by root systems decomposition [54], thereby indirectly increasing soil saturated hydraulic conductivity [47].

In our study, most of the attributes of soil macropores can positively influence soil hydraulic conductivity. This is because soil macropores can cause water to flow mainly through those macropores [56]. Previous studies confirmed that the most important prop-

erties of soil macropores explaining soil hydraulic conductivity are (1) the volume of percolating macropores, (2) the diameter of macropores, and (3) the number of macropores [57]. Hu et al. [13] and Borges et al. [58] revealed that soil macropore length density was significantly and positively correlated with soil hydraulic conductivity. Furthermore, soil hydraulic conductivity was also directly influenced by soil microporosity [13]. Decreased soil macroporosity and increased macropore tortuosity can cause decreased soil hydraulic conductivity [41]. High macropore volume confirmed that more water can flow through those macropores without any resistance—this is because soil macropores with high macropore volume can effectively discharge the air in soils and reduce the inhibition of air pressure on soil infiltration [59]. Meanwhile, soil macropores also increase lateral permeability and vertical infiltration, thus affecting soil hydraulic conductivity [59].

5. Conclusions

The values of total root length and total root volume were significantly larger at the large communities of reed than those at the small communities of reed ($p < 0.05$). Imaged macroporosity, macropore volume, macropore length density, macropore node density, macropore branch density, mean macropore surface area, mean macropore diameter, and mean macropore volume at the large communities of reed were significantly larger than those at the small communities of reed ($p < 0.05$), whereas mean macropore length, mean macropore branch length, and mean macropore tortuosity were the opposite. Total root length and total root volume were positively correlated with soil saturated hydraulic conductivity. Imaged macroporosity, macropore volume, macropore length density, macropore node density, macropore branch density, mean macropore surface area, mean macropore diameter, and mean macropore volume were positively correlated with soil saturated hydraulic conductivity, whereas mean macropore length, mean macropore branch length, and mean macropore tortuosity were negatively correlated with soil saturated hydraulic conductivity. This study was conducted using a small sample size, so future studies should be carried out on a larger-scale area and sample size both in space and time. Further, different soil types should also be considered in a future study.

Author Contributions: Conceptualization, Y.Z.; methodology, Y.Z.; software, Y.Z., W.Z. and L.W.; formal analysis, Y.Z., W.Z. and L.W.; investigation, Y.Z., W.Z. and L.W.; writing—original draft preparation, Y.Z.; writing—review and editing, Z.Z. and M.Z.; funding acquisition, M.Z. All authors have read and agreed to the published version of the manuscript.

Funding: This research was supported by the National Natural Science Foundation of China (41907007), Jiangsu Province Natural Science Foundation for Youth (BK20190747), and the National Natural Science Foundation of China (41771547).

Acknowledgments: The authors are grateful to the National Natural Science Foundation of China and Jiangsu Province Natural Science Foundation for Youth for financial support. We are highly thankful to the anonymous reviewers and editors for their careful reading and insightful comments and suggestions on our manuscript.

Conflicts of Interest: The authors of this manuscript declare that they have no competing interests or involvement in any organization or entity with any financial or nonfinancial interest in the subject matter or materials discussed in this manuscript.

References

1. Kochiieru, M.; Lamorski, K.; Feiza, V.; Feiziene, D.; Volungevicius, J. Quantification of the relationship between root parameters and soil macropore parameters under different land use systems in Retisol. *Int. Agrophysics* **2020**, *34*, 301–308. [CrossRef]
2. Chirol, C.; Spencer, K.L.; Carr, S.J.; Möller, I.; Evans, B.; Lynch, J.; Brooks, H.; Royse, K.R. Effect of vegetation cover and sediment type on 3D subsurface structure and shear strength in saltmarshes. *Earth Surf. Process. Landf.* **2021**, *46*, 2279–2297. [CrossRef]
3. Evans, B.; Brooks, H.; Chirol, C.; Kirkham, M.; Möller, I.; Royse, K.; Spencer, K.; Spencer, T. Vegetation interactions with geotechnical properties and erodibility of salt marsh sediments. *Estuar. Coast. Shelf Sci.* **2022**, *265*, 107713. [CrossRef]
4. Zhang, Y.H.; Chen, J.H.; Zhang, J.C.; Zhang, Z.; Zhang, M. Novel indicator for assessing wetland degradation based on the index of hydrological connectivity and its correlation with the root-soil interface. *Ecol. Indic.* **2021**, *133*, 108392. [CrossRef]

5. Engloner, A.I. Structure, growth dynamics and biomass of reed (Phragmites australis)–A review. *Flora-Morphol. Distrib. Funct. Ecol. Plants* **2009**, *204*, 331–346. [CrossRef]
6. Ghestem, M.; Sidle, R.C.; Stokes, A. The influence of plant root systems on subsurface flow: Implications for slope stability. *Bioscience* **2011**, *61*, 869–879. [CrossRef]
7. Hu, X.; Li, X.Y.; Wang, P.; Liu, Y.; Wu, X.C.; Li, Z.C.; Zhao, Y.D.; Cheng, Y.Q.; Guo, L.L.; Lyu, Y.L. Influence of exclosure on CT-measured soil macropores and root architecture in a shrub-encroached grassland in northern China. *Soil Tillage Res.* **2019**, *187*, 21–30. [CrossRef]
8. Chirol, C.; Carr, S.J.; Spencer, K.L.; Moeller, I. Pore, live root and necromass quantification in complex heterogeneous wetland soils using X-ray computed tomography. *Geoderma* **2021**, *387*, 114898. [CrossRef]
9. Bodner, G.; Leitner, D.; Kaul, H.-P. Coarse and fine root plants affect pore size distributions differently. *Plant Soil* **2014**, *380*, 133–151. [CrossRef]
10. Qiao, J.; Liu, X.; Zhu, Y.; Jia, X. Three-dimensional quantification of soil pore structure in wind-deposited loess under different vegetation types using industrial X-ray computed tomography. *Catena* **2021**, *199*, 105098. [CrossRef]
11. Wang, J.; Qin, Q.; Bai, Z. Characterizing the effects of opencast coal-mining and land reclamation on soil macropore distribution characteristics using 3D CT scanning. *Catena* **2018**, *171*, 212–221. [CrossRef]
12. Ben-Hur, M.; Yolcu, G.; Uysal, H.; Lado, M.; Paz, A. Soil structure changes: Aggregate size and soil texture effects on hydraulic conductivity under different saline and sodic conditions. *Soil Res.* **2009**, *47*, 688–696. [CrossRef]
13. Hu, X.; Li, X.Y.; Li, Z.C.; Gao, Z.; Wu, X.C.; Wang, P.; Lyu, Y.L.; Liu, L.Y. Linking 3-D soil macropores and root architecture to near saturated hydraulic conductivity of typical meadow soil types in the Qinghai Lake Watershed, northeastern Qinghai–Tibet Plateau. *Catena* **2020**, *185*, 104287. [CrossRef]
14. Pierret, A.; Capowiez, Y.; Belzunces, L.; Moran, C. 3D reconstruction and quantification of macropores using X-ray computed tomography and image analysis. *Geoderma* **2002**, *106*, 247–271. [CrossRef]
15. Luo, L.; Lin, H.; Halleck, P. Quantifying soil structure and preferential flow in intact soil using X-ray computed tomography. *Soil Sci. Soc. Am. J.* **2008**, *72*, 1058–1069. [CrossRef]
16. Archer, N.; Quinton, J.N.; Hess, T. Below-ground relationships of soil texture, roots and hydraulic conductivity in two-phase mosaic vegetation in South-east Spain. *J. Arid Environ.* **2002**, *52*, 535–553. [CrossRef]
17. Bodhinayake, W.; Cheng Si, B. Near-saturated surface soil hydraulic properties under different land uses in the St Denis National Wildlife Area, Saskatchewan, Canada. *Hydrol. Process.* **2004**, *18*, 2835–2850. [CrossRef]
18. Julich, S.; Kreiselmeier, J.; Scheibler, S.; Petzold, R.; Schwärzel, K.; Feger, K.-H. Hydraulic Properties of Forest Soils with Stagnic Conditions. *Forests* **2021**, *12*, 1113. [CrossRef]
19. Zhang, Y.; Huang, C.; Zhang, W.; Chen, J.; Wang, L. The concept, approach, and future research of hydrological connectivity and its assessment at multiscales. *Environ. Sci. Pollut. Res.* **2021**, *28*, 52724–52743. [CrossRef]
20. Bai, J.; Yu, Z.; Yu, L.; Wang, D.; Guan, Y.; Liu, X.; Gu, C.; Cui, B. In-situ organic phosphorus mineralization in sediments in coastal wetlands with different flooding periods in the Yellow River Delta, China. *Sci. Total Environ.* **2019**, *682*, 417–425. [CrossRef]
21. Zhang, J.M.; Xu, Z.M.; Li, F.; Hou, R.J.; Ren, Z. Quantification of 3D macropore networks in forest soils in Touzhai valley (Yunnan, China) using X-ray computed tomography and image analysis. *J. Mt. Sci.* **2017**, *14*, 474–491. [CrossRef]
22. Hu, X.; Li, Z.C.; Li, X.Y.; Liu, Y. Influence of shrub encroachment on CT-measured soil macropore characteristics in the Inner Mongolia grassland of northern China. *Soil Tillage Res.* **2015**, *150*, 1–9. [CrossRef]
23. Liu, B.; Fan, H.; Han, W.; Zhu, L.; Zhao, X.; Zhang, Y.; Ma, R. Linking soil water retention capacity to pore structure characteristics based on X-ray computed tomography: Chinese Mollisol under freeze-thaw effect. *Geoderma* **2021**, *401*, 115170. [CrossRef]
24. Ferreira, T.R.; Pires, L.F.; Wildenschild, D.; Heck, R.J.; Antonino, A.C. X-ray microtomography analysis of lime application effects on soil porous system. *Geoderma* **2018**, *324*, 119–130. [CrossRef]
25. Luo, L.; Lin, H.; Li, S. Quantification of 3-D soil macropore networks in different soil types and land uses using computed tomography. *J. Hydrol.* **2010**, *393*, 53–64. [CrossRef]
26. Peth, S.; Horn, R.; Beckmann, F.; Donath, T.; Fischer, J.; Smucker, A. Three-dimensional quantification of intra-aggregate pore-space features using synchrotron-radiation-based microtomography. *Soil Sci. Soc. Am. J.* **2008**, *72*, 897–907. [CrossRef]
27. Feng, Y.; Wang, J.; Bai, Z.; Reading, L.; Jing, Z. Three-dimensional quantification of macropore networks of different compacted soils from opencast coal mine area using X-ray computed tomography. *Soil Tillage Res.* **2020**, *198*, 104567. [CrossRef]
28. Gholizadeh-Sarabi, S.; Sepaskhah, A.R. Effect of zeolite and saline water application on saturated hydraulic conductivity and infiltration in different soil textures. *Arch. Agron. Soil Sci.* **2013**, *59*, 753–764. [CrossRef]
29. Ola, A.; Schmidt, S.; Lovelock, C.E. The effect of heterogeneous soil bulk density on root growth of field-grown mangrove species. *Plant Soil* **2018**, *432*, 91–105. [CrossRef]
30. Smith, K.D.; May, P.B.; Moore, G.M. The influence of compaction and soil strength on the establishment of four Australian landscape trees. *J. Arboric.* **2001**, *27*, 1–7. [CrossRef]
31. Cambi, M.; Hoshika, Y.; Mariotti, B.; Paoletti, E.; Picchio, R.; Venanzi, R.; Marchi, E. Compaction by a forest machine affects soil quality and Quercus robur L. seedling performance in an experimental field. *For. Ecol. Manag.* **2017**, *384*, 406–414. [CrossRef]
32. Yue, L.K.; Wang, Y.; Wang, L.; Yao, S.; Cong, C.; Ren, L.; Zhang, B. Impacts of soil compaction and historical soybean variety growth on soil macropore structure. *Soil Tillage Res.* **2021**, *214*, 105166. [CrossRef]

33. Colombi, T.; Torres, L.C.; Walter, A.; Keller, T. Feedbacks between soil penetration resistance, root architecture and water uptake limit water accessibility and crop growth—A vicious circle. *Sci. Total Environ.* **2018**, *626*, 1026–1035. [CrossRef]
34. Lipiec, J.; Horn, R.; Pietrusiewicz, J.; Siczek, A. Effects of soil compaction on root elongation and anatomy of different cereal plant species. *Soil Tillage Res.* **2012**, *121*, 74–81. [CrossRef]
35. Stewart, J.; Moran, C.; Wood, J. Macropore sheath: Quantification of plant root and soil macropore association. *Plant Soil* **1999**, *211*, 59–67. [CrossRef]
36. López-Bucio, J.; Cruz-Ramırez, A.; Herrera-Estrella, L. The role of nutrient availability in regulating root architecture. *Curr. Opin. Plant Biol.* **2003**, *6*, 280–287. [CrossRef]
37. Martínez, M.M.; Ortega, R.; Janssens, M.; Fincheira, P. Use of organic amendments in table grape: Effect on plant root system and soil quality indicators. *J. Soil Sci. Plant Nutr.* **2018**, *18*, 100–112. [CrossRef]
38. Kristoffersen, A.Ø.; Riley, H. Effects of soil compaction and moisture regime on the root and shoot growth and phosphorus uptake of barley plants growing on soils with varying phosphorus status. *Nutr. Cycl. Agroecosystems* **2005**, *72*, 135–146. [CrossRef]
39. Landl, M.; Huber, K.; Schnepf, A.; Vanderborght, J.; Javaux, M.; Glyn Bengough, A.; Vereecken, H. A new model for root growth in soil with macropores. *Plant Soil* **2017**, *415*, 99–116. [CrossRef]
40. Wang, M.; He, D.; Shen, F.; Huang, J.; Zhang, R.; Liu, W.; Zhu, M.; Zhou, L.; Wang, L.; Zhou, Q. Effects of soil compaction on plant growth, nutrient absorption, and root respiration in soybean seedlings. *Environ. Sci. Pollut. Res.* **2019**, *26*, 22835–22845. [CrossRef]
41. Colombi, T.; Braun, S.; Keller, T.; Walter, A. Artificial macropores attract crop roots and enhance plant productivity on compacted soils. *Sci. Total Environ.* **2017**, *574*, 1283–1293. [CrossRef]
42. Zhou, H.; Whalley, W.R.; Hawkesford, M.J.; Ashton, R.W.; Atkinson, B.; Atkinson, J.A.; Sturrock, C.J.; Bennett, M.J.; Mooney, S.J. The interaction between wheat roots and soil pores in structured field soil. *J. Exp. Bot.* **2021**, *72*, 747–756. [CrossRef]
43. Zhang, Y.H.; Jiang, J.; Zhang, J.C.; Zhang, Z.; Zhang, M. Effects of roots systems on hydrological connectivity below the soil surface in the Yellow River Delta wetland. *Ecohydrology* **2022**, *15*, e2393. [CrossRef]
44. Granse, D.; Titschack, J.; Ainouche, M.; Jensen, K.; Koop-Jakobsen, K. Subsurface aeration of tidal wetland soils: Root-system structure and aerenchyma connectivity in Spartina (Poaceae). *Sci. Total Environ.* **2022**, *802*, 149771. [CrossRef]
45. Jiang, X.J.; Liu, W.; Chen, C.; Liu, J.; Yuan, Z.-Q.; Jin, B.; Yu, X. Effects of three morphometric features of roots on soil water flow behavior in three sites in China. *Geoderma* **2018**, *320*, 161–171. [CrossRef]
46. Shi, X.; Qin, T.; Yan, D.; Tian, F.; Wang, H. A meta-analysis on effects of root development on soil hydraulic properties. *Geoderma* **2021**, *403*, 115363. [CrossRef]
47. Zhu, P.; Zhang, G.; Zhang, B. Soil saturated hydraulic conductivity of typical revegetated plants on steep gully slopes of Chinese Loess Plateau. *Geoderma* **2022**, *412*, 115717. [CrossRef]
48. Yu, Y.; Loiskandl, W.; Kaul, H.P.; Himmelbauer, M.; Wei, W.; Chen, L.; Bodner, G. Estimation of runoff mitigation by morphologically different cover crop root systems. *J. Hydrol.* **2016**, *538*, 667–676. [CrossRef]
49. Deguchi, T.; Iwama, K.; Matsumoto, M.; Tanigawa, J. Effect of varietal difference in root system on hydraulic conductance in potatoes under different soil water conditions and planting dates. *Potato Res.* **2015**, *58*, 103–119. [CrossRef]
50. Lu, J.; Zhang, Q.; Werner, A.D.; Li, Y.; Jiang, S.; Tan, Z. Root-induced changes of soil hydraulic properties–A review. *J. Hydrol.* **2020**, *589*, 125203. [CrossRef]
51. Nuttall, J.G.; Davies, S.; Armstrong, R.; Peoples, M. Testing the primer-plant concept: Wheat yields can be increased on alkaline sodic soils when an effective primer phase is used. *Aust. J. Agric. Res.* **2008**, *59*, 331–338. [CrossRef]
52. Gile, L.; Gibbens, R.; Lenz, J. Soils and sediments associated with remarkable, deeply-penetrating roots of crucifixion thorn (koeberlinia spinosazucc.). *J. Arid Environ.* **1995**, *31*, 137–151. [CrossRef]
53. Hao, H.X.; Wei, Y.J.; Cao, D.N.; Guo, Z.L.; Shi, Z.H. Vegetation restoration and fine roots promote soil infiltrability in heavy-textured soils. *Soil Tillage Res.* **2020**, *198*, 104542. [CrossRef]
54. Zhu, P.; Zhang, G.; Wang, H.; Xing, S. Soil infiltration properties affected by typical plant communities on steep gully slopes on the Loess Plateau of China. *J. Hydrol.* **2020**, *590*, 125535. [CrossRef]
55. De Baets, S.; Poesen, J.; Knapen, A.; Barberá, G.G.; Navarro, J. Root characteristics of representative Mediterranean plant species and their erosion-reducing potential during concentrated runoff. *Plant Soil* **2007**, *294*, 169–183. [CrossRef]
56. Ilek, A.; Kucza, J.; Witek, W. Using undisturbed soil samples to study how rock fragments and soil macropores affect the hydraulic conductivity of forest stony soils: Some methodological aspects. *J. Hydrol.* **2019**, *570*, 132–140. [CrossRef]
57. Cheik, S.; Bottinelli, N.; Minh, T.T.; Doan, T.T.; Jouquet, P. Quantification of three dimensional characteristics of macrofauna macropores and their effects on soil hydraulic conductivity in northern Vietnam. *Front. Environ. Sci.* **2019**, *7*, 31. [CrossRef]
58. Borges, J.A.; Pires, L.F.; Cássaro, F.A.; Auler, A.C.; Rosa, J.A.; Heck, R.J.; Roque, W.L. X-ray computed tomography for assessing the effect of tillage systems on topsoil morphological attributes. *Soil Tillage Res.* **2019**, *189*, 25–35. [CrossRef]
59. Beven, K.; Germann, P. Macropores and water flow in soils. *Water Resour. Res.* **1982**, *18*, 1311–1325. [CrossRef]